

Determining the molecular Huang-Rhys factor via STM induced luminescence

Fei Wen^{a)} and Guohui Dong^{b)†}

^{a)}Graduate School of China Academy of Engineering Physics, Beijing 100084, China

^{b)} College of Physics and Electronic Engineering, Sichuan Normal University, Chengdu 610068, China

The scanning tunneling microscopy induced luminescence (STML) can be used to probe the optical and electronic properties of molecules. Concerning the vibronic coupling, we model the molecule as a two-level system with the vibrational degrees of freedom. Based on the Bardeen's theory, we express the inelastic tunneling current in terms of Huang-Rhys factor within the inelastic electron scattering (IES) mechanism. We find that the differential conductance, varying with the bias voltage, exhibits distinct step structure with various vibronic coupling strength. The second derivative of the inelastic tunneling current with respect to the bias voltage shows the characteristics of vibrational-level structure with Franck-Condon factor. Consequently, we propose a method to determine the Huang-Rhys factor of molecules, holding promising potential within the realm of solid-state physics.

Keywords: scanning tunneling microscopy induced luminescences (STML), Franck-Condon factor, Huang-Rhys factor, inelastic electron scattering, differential conductance

1. Introduction

Scanning tunneling microscopy induced luminescence (STML) serves as a powerful tool for detecting various molecular properties, including molecular conformation [1, 2] and spectral characteristics [1–6]. Researchers have made substantial progresses in understanding the fine structures of molecular energy by combining the current-voltage characteristics of molecular

[†]Corresponding author, E-mail: 20210076@sicnu.edu.cn

junctions with optical spectroscopy [7–14]. Intramolecular transitions with vibronic features have also been successfully detected in the differential conductance spectra at the threshold of a vibrational mode energy [2, 15–20].

In 1950, Huang and co-workers derived the expression for the Huang-Rhys factor (denoted as S) which characterizes the strength of the vibronic coupling [21]. The critical importance of the Huang-Rhys factor was confirmed in both theory and experiments [22–25]. Although a simple model which assumes that all vibration modes have the same frequency under the Born-Oppenheimer approximation is used. In many practical applications, the results derived from this simplest model have been proven to be the most useful. There are several ways to determine the Huang-Rhys factor in experiments, such as fitting the spectrum and extracting S from the Stokes shift. However, these methods often require accurate spectral shapes and higher resolution, which can be challenging to achieve in practice [26]. Taking advantage of the low temperature and excellent accuracy of STML, measuring the Huang-Rhys factor becomes a more accessible task.

In general, the luminescence is induced by STM with three mechanisms: the inelastic electron scattering (IES) mechanism [7, 27–33], charge injection (CI) mechanism [2, 11, 34–37] and the plasmon mechanism [12, 38–41]. Here, we specifically focus on the IES mechanism, where electrons tunnel inelastically from one electrode to another, exciting the molecule in the gap of the tip and the substrate. Taking the vibronic coupling into account, we calculate the inelastic tunneling current based on the perturbation theory [42]. The inelastic tunneling current is expressed in terms of the Franck-Condon factor which describes the square of the overlap integral between the vibrational wave functions of the two states that are involved in the transition. The Franck-Condon factor is written in the form of the Huang-Rhys factor [43, 44], which is determined through the second derivative of the inelastic tunneling current with respect to the bias voltage.

The rest of the paper is organized as follows. In section 2 we describe the Hamiltonian of our model in which the molecule is treated as a two-level system with the vibration degree of the freedom. Then, we derive the inelastic tunneling current in terms of Huang-Rhys factor. Section 3 shows the inelastic tunneling current, the differential conductance and the second

derivative of the inelastic tunneling current with respect to the bias voltage as a function of the bias voltage. Finally, we summarize the main contributions in section 4.

2. Model and method

2.1. Hamiltonian

The STML system comprises a metallic tip, a molecular sample, a decoupling layer and a metallic substrate. The decoupling layer serves to separate the molecule from the substrate, blocking the quenching process and enabling the molecular luminescence. In the IES mechanism, when a bias voltage is applied between the tip and substrate, electrons tunnel from one electrode to another, thereby exciting the molecule.

The total Hamiltonian is divided into three components: the electronic Hamiltonian, the molecular Hamiltonian and the interaction Hamiltonian. The electronic component is solved by Bardeen's theory. The molecular aspect is simplified as a two-level system with vibrational degrees of freedom. The interaction between the electron and the molecule is Coulomb interaction.

Based on Bardeen's theory, it is assumed that the tip and the substrate are separated from each other. The stationary Schrödinger equations are

$$\hat{H}_t |\phi_k\rangle = \tilde{\xi}_k |\phi_k\rangle, \quad (1)$$

$$\hat{H}_s |\varphi_n\rangle = \tilde{E}_n |\varphi_n\rangle, \quad (2)$$

where \hat{H}_t and \hat{H}_s represent the Hamiltonians of electrons in the tip and the substrate respectively. ϕ_k and φ_n are the electronic wave function of the corresponding region. $\tilde{\xi}_k$ and \tilde{E}_n are the energies of the tunneling electrons located at the tip and the substrate region when the bias voltage V_b is applied between the electrodes. $\tilde{\xi}_k$ and \tilde{E}_n are expressed in terms of the electronic energy in the absence of the bias voltage,

$$\tilde{\xi}_k = \xi_k + eV_b, \quad (3)$$

$$\tilde{E}_n = E_n, \quad (4)$$

where ξ_k (E_n) is the energy of the tunneling electron at the tip (substrate) when the bias is zero. e represents the elementary charge of an electron. Selecting the center of the molecule as the origin of the coordinates, the wave functions in Eq. 1 and Eq. 2 are explicitly written as

$$\phi_k(\vec{r}) = A_k \frac{e^{-\kappa_k(|\vec{r}-\vec{a}|-R)}}{\kappa_k |\vec{r}-\vec{a}|}, \quad (5)$$

$$\varphi_n(\vec{r}) = B_n e^{-\kappa_n|z|}, \quad (6)$$

in which A_k and B_n are the normalized coefficients. \vec{r} represents the position of the tunneling electron. $|z|$ denotes the distance between the tunneling electron and the substate. The apex of the tip is assumed to be sphere. The coordinates of the center and the radius of curvature are denoted as \vec{a} and R . κ_k and κ_n are the decay constants and can be expressed as

$$\kappa_k = \frac{\sqrt{-2m_e\xi_k}}{\hbar}, \quad (7)$$

$$\kappa_n = \frac{\sqrt{-2m_e E_n}}{\hbar}, \quad (8)$$

in which m_e represents the mass of the electron and \hbar is the reduced Plank constant.

The molecule is modeled as a two-level system with the vibrational degrees of freedom. The molecular Hamiltonian is

$$\hat{H}_m = (E_g + \nu_g \hbar \omega) |g, \nu\rangle \langle g, \nu| + (E_e + \nu' \hbar \omega) |e, \nu'\rangle \langle e, \nu'|, \quad (9)$$

where ω is the frequency of vibration. E_g and $\nu \hbar \omega$ (E_e and $\nu' \hbar \omega$) represent the electronic energy and the vibrational energy associated with the ground (excited) state of the molecular. $|g\rangle$ represents the ground state of the molecular electron, while $|e\rangle$ corresponds to the excited state. $|\nu\rangle$ ($|\nu'\rangle$) is the vibrational state with the ground (excited) state of the molecule.

The interaction is approximated as the electron-dipole interaction [32],

$$\hat{H}_{el-m} = -e \frac{\vec{r} \cdot \vec{\mu}}{|\vec{r}|^3}, \quad (10)$$

where $\vec{\mu}$ is the molecular dipole.

2.2. The Franck-Condon factor

Within the Born-Oppenheimer approximation, the total wave function of the molecule is expressed as the product of the electronic wave function and the vibrational wave function. For the treatment of molecular vibrations, the harmonic approximation is often employed. The Hamiltonian of the nuclear vibration takes the form of a harmonic oscillator [21] with the characteristic frequency ω . The ground states of vibrational states $|\nu\rangle$ and $|\nu'\rangle$ can be expressed as $|0_g\rangle$ and $|0_e\rangle$, respectively. The subscript g and e indicate the electronic ground state and excited state that couple with vibrational states. In the molecular excited state, the harmonic oscillation is viewed as a translation of the harmonic oscillator when the molecule is in the ground state, thus we establish the following relationship:

$$|0_e\rangle = \hat{D}(\alpha) |0_g\rangle, \quad (11)$$

in which $\hat{D}(\alpha)$ is the translation operator, capable of translating the harmonic oscillator by a distance of q in real space.

$$q = \alpha \sqrt{\frac{2\hbar}{m_n \omega}}, \quad (12)$$

where m_n is the mass of the harmonic oscillation. The Franck-Condon factor describes the overlap of the vibrational wave function in the molecular ground state and the molecular excited state. It is expressed as follows:

$$F_{\nu\nu'} = |\langle \nu | \nu' \rangle|^2. \quad (13)$$

Due to the low temperature of the experiment, the vibrational state associated with the electronic ground state is assumed to be in its ground state, i.e., $|\nu\rangle = |0_g\rangle$. Then, the Franck-Condon factor is simplified as

$$|\langle 0_g | \nu' \rangle|^2 = e^{-S} \frac{S^{\nu'}}{\nu'!}, \quad (14)$$

where S is the Huang-Rhys factor and it can be expressed as

$$S = |\alpha|^2 = q^2 \frac{m_n \omega}{2\hbar}. \quad (15)$$

2.3. The inelastic tunneling current

At the initial time, we assume that the tunneling electron is located in the substrate region and the molecule is in the electronic and vibrational ground state due to the low temperature in experiments. We express the state of the system at time t as

$$|\Psi(t)\rangle = e^{-i(\tilde{E}_n + E_g + \nu_g \hbar\omega)t/\hbar} |g, \nu\rangle |\varphi_n\rangle + \sum_{k,\nu} c_{g\nu k}(t) |g, \nu\rangle |\phi_k\rangle + \sum_{k,\nu'} c_{e\nu' k}(t) |e, \nu'\rangle |\phi_k\rangle,$$

where $|\nu\rangle = |0_g\rangle$. $c_{g\nu k}$ represents the elastic tunneling amplitude, while $c_{e\nu' k}$ signifies the inelastic tunneling amplitude. Since the molecular vibration does not contribute to the elastic current, we research the inelastic tunneling process only. By solving the time-dependent Schrödinger equation, we derive the inelastic tunneling current as follows:

$$I_{s,t} = \frac{2\pi e}{\hbar} \sum_{\nu, \nu'} \int_{-\infty}^{\mu_0} dE_n \int_{\mu_0}^0 d\xi_k \rho_s(E_n) \rho_t(\xi_k) \mathcal{N}_{s,t}^2 |_{E_n \rightarrow \xi_k} \times \langle \nu | \nu' \rangle^2 \delta [E_{eg} + (\nu' - \nu) \hbar\omega + \xi_k + eV_b - E_n], \quad (16)$$

where μ_0 is the Fermi level of electrodes, with the assumption that the tip and the substrate are composed of the same metal. ρ_s and ρ_t denote the energy density of the substrate and the tip, respectively. E_{eg} is the energy gap of the molecule. $\mathcal{N}_{s,t} |_{E_n \rightarrow \xi_k}$ represents the inelastic tunneling matrix element describing the process of the electrons tunneling from the substrate to the tip. It is written as follows:

$$\mathcal{N}_{s,t} |_{E_n \rightarrow \xi_k} = -e\vec{\mu} \cdot \langle \phi_k | \frac{\vec{r}}{|\vec{r}|^3} | \varphi_n \rangle. \quad (17)$$

Substituting the expression of the Franck-Condon factor into Eq. 16, we derive the expression of the inelastic current

$$I_{s,t} = \frac{2\pi e}{\hbar} \sum_{\nu'} e^{-S} \frac{S^{\nu'}}{\nu'!} \int_{-\infty}^{\mu_0} dE_n \int_{\mu_0}^0 d\xi_k \rho_s(E_n) \rho_t(\xi_k) \times \mathcal{N}_{s,t}^2 |_{E_n \rightarrow \xi_k} \delta (E_{eg} + \nu' \hbar\omega + \xi_k + eV_b - E_n). \quad (18)$$

This expression can be simplified due to the δ function. For convenience, we introduce the following definition:

$$\Delta = E_{eg} + \nu' \hbar\omega + eV_b. \quad (19)$$

Thus, the range of the integral alters with the value of Δ . When $\mu_0 < \Delta < 0$, the current is written as

$$I_{s,t} = \frac{2\pi e}{\hbar} \sum_{\nu'} e^{-S} \frac{S^{\nu'}}{\nu'!} \int_{\mu_0}^{\mu_0 - \Delta} d\xi_k \rho_s(\xi_k + \Delta) \rho_t(\xi_k) \mathcal{N}_{s,t}^2 |_{\xi_k + \Delta \rightarrow \xi_k}, \quad (20)$$

When $\Delta < \mu_0$, the current becomes

$$I_{s,t} = \frac{2\pi e}{\hbar} \sum_{\nu'} e^{-S} \frac{S^{\nu'}}{\nu'!} \int_{\mu_0}^0 d\xi_k \rho_s(\xi_k + \Delta) \rho_t(\xi_k) \mathcal{N}_{s,t}^2 |_{\xi_k + \Delta \rightarrow \xi_k}. \quad (21)$$

In experiments, both the elastic and the inelastic mechanism contribute to the current spectrum. We can obtain the inelastic component via the luminescence from the molecule. Once the molecule is excited to its excited state, it then decays back through the spontaneous emission process. We denote the photon-counting rate as $p_e(t)$. The master equation of the molecule excited state reads [32]

$$\frac{dp_e(t)}{dt} = -\gamma p_e(t) + \frac{I_{s,t}}{e}, \quad (22)$$

in which γ is the spontaneous decay rate. In the steady state, the photon-counting rate becomes

$$\Gamma = \frac{I_{s,t}}{e}. \quad (23)$$

Thus the inelastic tunneling current can be obtained from the photon-counting spectrum.

3. Results

3.1. The inelastic tunneling current and the differential conductance

For numerical calculations of the inelastic tunneling current, we select the silver (Ag) as the material for both the tip and the substrate. The Fermi level of silver is -4.64eV . The characteristic frequency of the molecular vibration is assumed to be 0.1eV . The distance between the tip and the substrate is set to $d = 0.5\text{nm}$ and the radius of the apex atom of the tip is 0.5nm . The tip is placed above the molecule. Taking the symmetry of the system into account, we express the position of the tip's apex as $\vec{a} = (0, 0, d + R)$. Furthermore, we choose

different vibrational quantum numbers for the electronic excited state, ranging from 0 to 10. We also consider various cases with S equal to 0.1, 1 and 10, indicating weak coupling, medium coupling and strong coupling between the vibration and electrons, respectively.

The Fig. 3. illustrates the behavior of the inelastic tunneling current (top figures) and the differential conductance (bottom figures) varying with respect to the bias voltage. The inelastic tunneling current increases as the bias voltage increases. The onset bias voltage differs among Fig. 3.1(a), (b) and (c), because the vibronic coupling alters the molecular energy gap. Due to the Franck-Condon principle, a transition from one vibrational energy level to another is more likely to occur if the two vibrational wave functions overlap significantly. The effective bias voltage is given by $eV_{eff} = -E_{eg} - [S] \hbar\omega$, where $[S]$ is the floor function and expressed as $[S] = \max \{n \in \mathbb{Z} \mid n \leq S\}$. The curves of the differential conductance in Fig. 3.1(d), (e) and (f) exhibit steps structures. The spacing between these steps corresponds to the characteristic frequency $\hbar\omega$ of the molecular vibration.

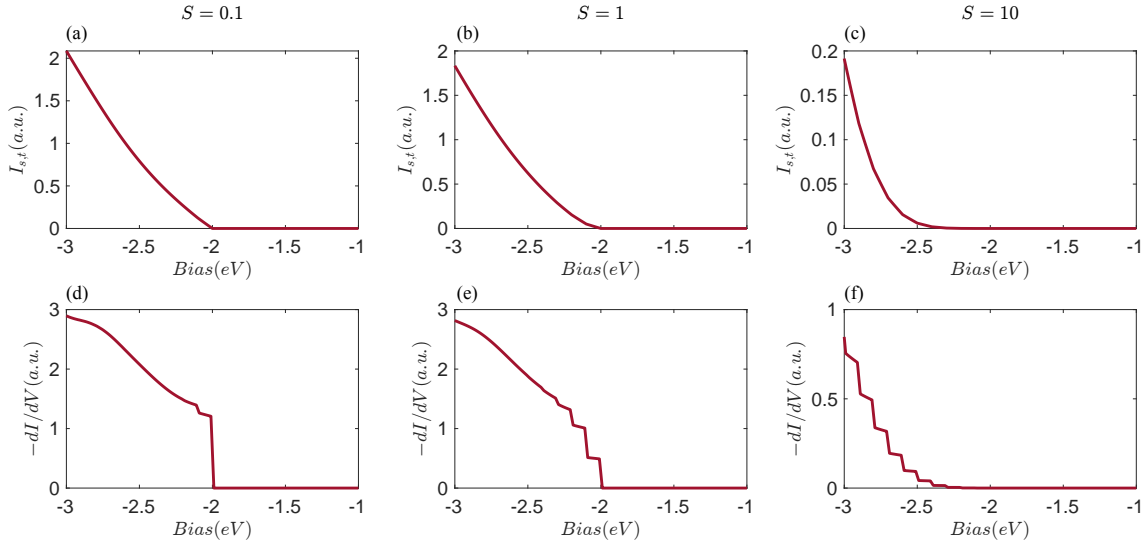


Fig.1. (a)-(c) The inelastic tunneling current as a function of the bias voltage with $S = 0.1$, $S = 1$ and $S = 10$, respectively. (d)-(f) The differential conductance as a function of the bias voltage with $S = 0.1$, $S = 1$ and $S = 10$, respectively. The characteristic frequency of the molecular vibration is fixed at 0.1eV.

3.2. Determining the Huang-Rhys factor

The red lines in Fig. 3.2 illustrate the normalized second derivative of the inelastic tunneling current with respect to the bias voltage. Fig. 3.2(a), (b) and (c) correspond to the parameter with $S = 0.1$, $S = 1$ and $S = 10$, respectively. These peaks in the graph represent the contribution of the vibration to the inelastic tunneling current. The blue circles represent the normalized values of the Franck-Condon factor for integer values of ν varying from 0 to 10. The blue line connects these circles in sequence. For small values of ν , such as $\nu = 0$ and $\nu = 1$, the intensity of these peaks matches with blue circles and the envelope of these peaks is consistent with the blue line very well. Thus, for a given Huang-Rhys factor, the Franck-Condon factor effectively presents the character of the intensity of the second derivative of the inelastic tunneling current concerning the bias voltage.

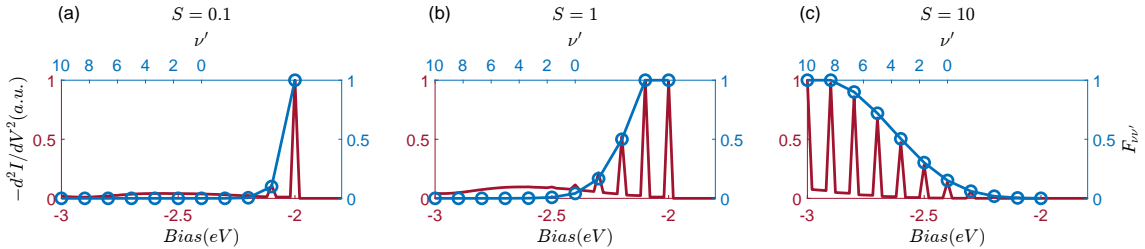


Fig.2. The second derivative of the inelastic tunneling current with respect to the bias voltage (red) and the Frank-Condon factor (blue) as a function of the bias voltage. (a)-(c) correspond to the case of $S = 0.1$, $S = 1$ and $S = 10$, respectively.

From the expression of the inelastic tunneling current in Eq. (18), we can decompose $d^2I_{s,t}/dV^2$ with the vibronic quantum number ν' , and define $(d^2I_{s,t}/dV^2)_{\nu'}$ of the ν' -th order as

$$(d^2I_{s,t}/dV^2)_{\nu'} = e^{-S} \frac{S^{\nu'}}{\nu'!} D_{\nu'}. \quad (24)$$

Here, we have the expression of the factor $D_{\nu'}$,

$$\begin{aligned} D_{\nu'} &= \frac{2\pi e}{\hbar} \frac{d^2}{dV^2} \int_{-\infty}^{\mu_0} dE_n \int_{\mu_0}^0 d\xi_k \rho_s(E_n) \rho_t(\xi_k) \\ &\times \mathcal{N}_{s,t}^2 |_{E_n \rightarrow \xi_k} \delta(E_{eg} + \nu' \hbar\omega + \xi_k + eV_b - E_n). \end{aligned} \quad (25)$$

When the factor $D_{\nu'}$ changes with ν' as a slowly varying function, we get an approximate result about the ν' -th order and the $(\nu' - 1)$ -th order of $d^2I_{s,t}/dV^2$ as

$$\frac{(d^2I_{s,t}/dV^2)_{\nu'}}{(d^2I_{s,t}/dV^2)_{\nu'-1}} \approx \frac{S}{\nu'}, \quad (26)$$

especially [45, 46]

$$\frac{(d^2I_{s,t}/dV^2)_1}{(d^2I_{s,t}/dV^2)_0} \approx S, \quad (27)$$

The ratio of the intensity of the first-order $d^2I_{s,t}/dV^2$ to the zero order $d^2I_{s,t}/dV^2$ is approximately equal to the Huang-Rhys factor. This conclusion provides a theoretical foundation for our experimental determination of the Huang-Rhys factor: Once the inelastic tunneling current is obtained, we can analyze its second derivative with respect to the bias voltage., from which the oscillation quantum number ν' can be obtained. Also, the interval between peaks can give the value of the vibronic frequency ω . Through intensity of these peaks with the first order and the zero order, we calculate the Huang-Rhys factor.

To verify the validity of the method for determining the Huang-Rhys factor through the second derivative inelastic tunneling current, Fig. 3 illustrates the results estimated from Eq.(27) as a function of the true value of S . The red line is linear and represent the true value of S . The blue circles are the estimated values from Eq. 27 with different vibronic coupling strength , corresponding cases of $S = 0.1$, $S = 0.5$, $S = 1$, $S = 5$ and $S = 10$, respectively. There is a slight difference between the estimated value and the true values in the case of weak vibronic coupling. However, in the cases of the strong vibronic coupling, the estimated S matches the true S very well. This figure shows that $D_{\nu'}$ is a slowly varying function, and Eq. 27 can be used to determine the Huang-Rhys factor of the molecule.

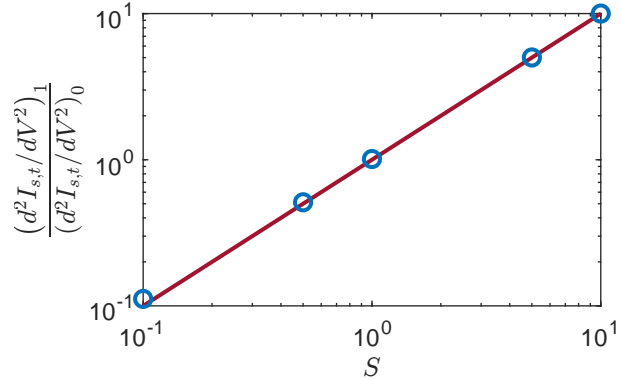


Fig.3. The comparison of the estimated value from Eq. 27 with the true value. The red line is linear and represents the true value of S . The blue circles are the estimated values from the left hand of Eq. 27, corresponding cases of $S = 0.1$, $S = 0.5$, $S = 1$, $S = 5$ and $S = 10$, respectively.

4. Conclusion

We have studied the STML system, where the molecule is modeled as the two-level system with a molecular vibration degree of freedom. Based on Bardeen’s theory, the inelastic tunneling current is expressed in terms of Huang-Rhys factor S . Information regarding vibronic coupling is obtained from the differential conductance, which exhibits steps as a function of the bias voltage. The Huang-Rhys factor is determined from the second derivative of the inelastic tunneling current with respect to the bias voltage. The method involving the analysis of the inelastic tunneling current in STML will provide an alternative approach for determining the Huang-Rhys factor.

Acknowledgments

This work is supported by the National Natural Science Foundation of China (NSFC) (Grant Nos. 11 875 049 and 12205211), the NSAF (Grant Nos. U1730449 and U1930403), and the National Basic Research Program of China (Grant No. 2016YFA0301201).

References

- [1] X. H. Qiu, G. V. Nazin, and W. Ho. Vibrationally resolved fluorescence excited with submolecular precision. *Science*, 299(5606):542–546, jan 2003.
- [2] F. Schwarz, Y. F. Wang, W. A. Hofer, R. Berndt, E. Runge, and J. Kröger. Electronic and vibrational states of single tin–phthalocyanine molecules in double layers on Ag(111). *J. Phys. Chem. C*, 119(27):15716–15722, jun 2015.
- [3] X. H. Qiu, G. V. Nazin, and W. Ho. Vibronic states in single molecule electron transport. *Phys. Rev. Lett.*, 92(20):206102, may 2004.
- [4] S. W. Wu, N. Ogawa, G. V. Nazin, and W. Ho. Conductance hysteresis and switching in a single-molecule junction. *J. Phys. Chem. C*, 112(14):5241–5244, feb 2008.
- [5] Chi Chen, Ping Chu, C. A. Bobisch, D. L. Mills, and W. Ho. Viewing the interior of a single molecule: Vibronically resolved photon imaging at submolecular resolution. *Phys. Rev. Lett.*, 105(21):217402, nov 2010.
- [6] Yang Zhang, Yang Luo, Yao Zhang, Yun-Jie Yu, Yan-Min Kuang, Li Zhang, Qiu-Shi Meng, Yi Luo, Jin-Long Yang, Zhen-Chao Dong, and J. G. Hou. Visualizing coherent intermolecular dipole–dipole coupling in real space. *Nature*, 531(7596):623–627, mar 2016.
- [7] Tadahiro Komeda. Chemical identification and manipulation of molecules by vibrational excitation via inelastic tunneling process with scanning tunneling microscopy. *Prog. Surf. Sci.*, 78(2):41–85, jan 2005.
- [8] Satoshi Katano, Sukekatsu Ushioda, and Yoichi Uehara. Vibrational excitation of a single benzene molecule adsorbed on Cu(110) studied by scanning tunneling microscope light emission spectroscopy. *J. Phys. Chem. Lett.*, 1(19):2763–2768, sep 2010.
- [9] N. Jiang, E. T. Foley, J. M. Klingsporn, M. D. Sonntag, N. A. Valley, J. A. Dieringer, T. Seideman, G. C. Schatz, M. C. Hersam, and R. P. Van Duyne. Observation of multiple vibrational modes in ultrahigh vacuum tip-enhanced raman spectroscopy combined with molecular-resolution scanning tunneling microscopy. *Nano Lett.*, 12(10):5061–5067, jan 2012.

- [10] Li Zhang, Yun-Jie Yu, Liu-Guo Chen, Yang Luo, Ben Yang, Fan-Fang Kong, Gong Chen, Yang Zhang, Qiang Zhang, Yi Luo, Jin-Long Yang, Zhen-Chao Dong, and J. G. Hou. Electrically driven single-photon emission from an isolated single molecule. *Nat. Commun.*, 8(1), sep 2017.
- [11] Kuniyuki Miwa, Hiroshi Imada, Miyabi Imai-Imada, Kensuke Kimura, Michael Galperin, and Yousoo Kim. Many-body state description of single-molecule electroluminescence driven by a scanning tunneling microscope. *Nano Lett.*, 19(5):2803–2811, jan 2019.
- [12] Fan-Fang Kong, Xiao-Jun Tian, Yang Zhang, Yun-Jie Yu, Shi-Hao Jing, Yao Zhang, Guang-Jun Tian, Yi Luo, Jin-Long Yang, Zhen-Chao Dong, and J. G. Hou. Probing intramolecular vibronic coupling through vibronic-state imaging. *Nat. Commun.*, 12(1), feb 2021.
- [13] Ricardo Javier Peña Román, Delphine Pommier, Rémi Bretel, Luis E. Parra López, Etienne Lorchat, Julien Chaste, Abdelkarim Ouerghi, Séverine Le Moal, Elizabeth Boer-Duchemin, Gérald Dujardin, Andrey G. Borisov, Luiz F. Zagonel, Guillaume Schull, Stéphane Berciaud, and Eric Le Moal. Electroluminescence of monolayer WS₂ in a scanning tunneling microscope: Effect of bias polarity on spectral and angular distribution of emitted light. *Phys. Rev. B*, 106(8):085419, aug 2022.
- [14] Fei Wen, Guohui Dong, and Hui Dong. Measuring fine molecular structures with luminescence signal from an alternating current scanning tunneling microscope. *Commun. Theor. Phys.*, 74(12):125105, nov 2022.
- [15] B. C. Stipe, M. A. Rezaei, and W. Ho. Single-molecule vibrational spectroscopy and microscopy. *Science*, 280(5370):1732–1735, jun 1998.
- [16] B. C. Stipe, M. A. Rezaei, and W. Ho. Coupling of vibrational excitation to the rotational motion of a single adsorbed molecule. *Phys. Rev. Lett.*, 81(6):1263–1266, aug 1998.
- [17] L. J. Lauhon and W. Ho. Single-molecule vibrational spectroscopy and microscopy: CO on Cu(001) and Cu(110). *Phys. Rev. B*, 60(12):R8525–R8528, sep 1999.
- [18] N. Lorente and M. Persson. Theory of single molecule vibrational spectroscopy and microscopy. *Phys. Rev. Lett.*, 85(14):2997–3000, Oct 2000.
- [19] Nilay A. Pradhan, Ning Liu, and Wilson Ho. Vibronic spectroscopy of single C₆₀ molecules and monolayers with the STM. *J. Phys. Chem. B*, 109(17):8513–8518, feb 2005.

- [20] G. V. Nazin, S. W. Wu, and W. Ho. Tunneling rates in electron transport through double-barrier molecular junctions in a scanning tunneling microscope. *Proc. Natl. Acad. Sci.*, 102(25):8832–8837, jun 2005.
- [21] Kun Huang, Avril Rhys, and Nevill Francis Mott. Theory of light absorption and non-radiative transitions in F-centres. *Proc. R. Soc. Lond. A*, 204(1078):406–423, 1950.
- [22] Anthony M. Lemos and Jordan J. Markham. Calculation of the Huang-Rhys factor for F-centers. *J. Phys. Chem. Solids*, 26(12):1837–1851, dec 1965.
- [23] E. Mulazzi and Nice Terzi. Evaluation of the Huang-Rhys factor and the half-width of the F-band in KCl and NaCl crystals. *J. Phys. Colloques*, 28(C4), aug 1967.
- [24] M Moreno, M T Barriuso, and J A Aramburu. The Huang-Rhys factor $S(a1g)$ for transition-metal impurities: a microscopic insight. *J. Phys.: Condens. Matter*, 4(47):9481, nov 1992.
- [25] A. Schenk. A model for the field and temperature dependence of Shockley-Read-Hall lifetimes in silicon. *Solid-State Electron.*, 35(11):1585–1596, nov 1992.
- [26] Mathijs de Jong, Luis Seijo, Andries Meijerink, and Freddy T. Rabouw. Resolving the ambiguity in the relation between Stokes shift and Huang–Rhys parameter. *Phys. Chem. Chem. Phys. PCCP*, 17(26):16959–16969, 2015.
- [27] N. Mingo and K. Makoshi. Calculation of the inelastic scanning tunneling image of acetylene on Cu(100). *Phys. Rev. Lett.*, 84(16):3694–3697, apr 2000.
- [28] S. Tikhodeev, M. Natario, K. Makoshi, T. Mii, and H. Ueba. Contribution to a theory of vibrational scanning tunneling spectroscopy of adsorbates. *Surf. Sci.*, 493(1-3):63–70, nov 2001.
- [29] Takashi Mii, Sergei Tikhodeev, and Hiromu Ueba. Theory of vibrational tunneling spectroscopy of adsorbates on metal surfaces. *Surf. Sci.*, 502-503:26–33, apr 2002.
- [30] Aaron Hurley, Nadjib Baadji, and Stefano Sanvito. Spin-flip inelastic electron tunneling spectroscopy in atomic chains. *Phys. Rev. B*, 84(3):035427, jul 2011.
- [31] Fabian Eickhoff, Elena Kolodzeiski, Taner Esat, Norman Fournier, Christian Wagner, Thorsten Deilmann, Ruslan Temirov, Michael Rohlffing, F. Stefan Tautz, and Frithjof B. Anders. Inelastic

electron tunneling spectroscopy for probing strongly correlated many-body systems by scanning tunneling microscopy. *Phys. Rev. B*, 101(12):125405, mar 2020.

[32] Guohui Dong, Yining You, and Hui Dong. Microscopic origin of molecule excitation via inelastic electron scattering in scanning tunneling microscope. *New J. Phys.*, 22(11):113010, nov 2020.

[33] Guohui Dong, Zhubin Hu, Xiang Sun, and Hui Dong. Structural reconstruction of optically invisible state in a single molecule via scanning tunneling microscope. *J. Phys. Chem. Lett.*, 12(41):10034–10039, oct 2021.

[34] D. Drakova and G. Doyen. Local charge injection in STM as a mechanism for imaging with anomalously high corrugation. *Phys. Rev. B*, 56(24):R15577–R15580, dec 1997.

[35] Michael Galperin and Abraham Nitzan. Current-induced light emission and light-induced current in molecular-tunneling junctions. *Phys. Rev. Lett.*, 95(20):206802, nov 2005.

[36] Upendra Harbola, Jeremy B. Maddox, and Shaul Mukamel. Many-body theory of current-induced fluorescence in molecular junctions. *Phys. Rev. B*, 73(7):075211, feb 2006.

[37] Song Jiang, Tomáš Neuman, Rémi Bretel, Alex Boeglin, Fabrice Scheurer, Eric Le Moal, and Guillaume Schull. Many-body description of STM-induced fluorescence of charged molecules. *Phys. Rev. Lett.*, 130(12):126202, mar 2023.

[38] Benjamin Doppagne, Michael C. Chong, Etienne Lorchat, Stéphane Berciaud, Michelangelo Romeo, Hervé Bulou, Alex Boeglin, Fabrice Scheurer, and Guillaume Schull. Vibronic spectroscopy with submolecular resolution from STM-induced electroluminescence. *Phys. Rev. Lett.*, 118(12):127401, mar 2017.

[39] Alberto Martín-Jiménez, Antonio I. Fernández-Domínguez, Koen Lauwaet, Daniel Granados, Rodolfo Miranda, Francisco J. García-Vidal, and Roberto Otero. Unveiling the radiative local density of optical states of a plasmonic nanocavity by STM. *Nat. Commun.*, 11(1), feb 2020.

[40] Jia-Zhe Zhu, Gong Chen, Talha Ijaz, Xiao-Guang Li, and Zhen-Chao Dong. Influence of an atomistic protrusion at the tip apex on enhancing molecular emission in tunnel junctions: A theoretical study. *J. Chem. Phys.*, 154(21), jun 2021.

- [41] Kuniyuki Miwa, Souichi Sakamoto, and Akihito Ishizaki. Control and enhancement of single-molecule electroluminescence through strong light–matter coupling. *Nano Lett.*, 23(8):3231–3238, apr 2023.
- [42] J. Bardeen. Tunnelling from a Many-Particle Point of View. *Phys. Rev. Lett.*, 6(2):57–59, jan 1961.
- [43] J. Franck and E. G. Dymond. Elementary processes of photochemical reactions. *Trans. Faraday Soc.*, 21(February):536, 1926.
- [44] Edward Condon. A Theory of Intensity Distribution in Band Systems. *Phys. Rev.*, 28(6):1182–1201, dec 1926.
- [45] S. J. Xu, W. Liu, and M. F. Li. Direct determination of free exciton binding energy from phonon-assisted luminescence spectra in GaN epilayers. *Appl. Phys. Lett.*, 81(16):2959–2961, oct 2002.
- [46] Shi-Jie Xu. Huang-Rhys factor and its key role in the interpretation of some optical properties of solids. *Acta Phys. Sin-ch. Ed.*, 68(16):166301, 2019.